DIFFUSION KINETICS OF BORON IN THE X200CrMoV12 HIGH-ALLOY STEEL

O. Azouani [a], **M. Keddam** [b,*], **A. Brahimi** [c], **A. Sehisseh** [a]

[a] Commissariat à l'Energie Atomique, Centre de Recherche Nucléaire de Draria (CRND),
Draria, Algiers, Algeria
[b] USTHB, Faculté de Génie Mécanique et Génie des Procédés, Laboratoire de Technologie
des Matériaux, Département SDM, Algiers, Algeria
[c] Laboratoire de Traitement de Surface et Matériaux, Département de Génie Mécanique,
Université Saad Dahlab, Route De Soumaa, Algeria.

Abstract

In this work, the kinetics of the boride layers (FeB/Fe2B), formed on the X200CrMoV12 steel used for the cold-working, was investigated. The boriding treatment was carried out in the powder mixture consisting of 5%B_4C, 5% $NaBF_4$ and 90% SiC.
The boriding parameters are : 900, 950 and 1000°C with treatment times of 2, 4 and 6 h. The obtained borided layers (FeB/Fe_2B) were characterized by the following experimental techniques: optical microscopy, scanning electron microscopy coupled to EDS analysis and XRD analysis. The kinetics of boron diffusion in the X200CrMoV12 steel was also studied. As a result, the time dependence of the borided layers thicknesses followed a growth parabolic law. The boron activation energy was estimated as 199.37 kJ mol^{-1} for the X200CrMoV12 steel. A full factorial design with 2 factors at 3 levels was employed to estimate the total boride layer thickness as a function of the boriding parameters (time and temperature) and a simple equation was proposed. Finally, an iso-thickness diagram was given as a tool to predict the total boride layers thicknesses in relation with the practical utilization of this kind of steel.

Keywords: Boriding; Diffusion; Iron borides; Kinetics; Activation energy; Regression model

1. Introduction.

Boriding is a thermo-chemical process, which involves diffusion of boron atoms into the surface of ferrous alloys to form a hard layer consisting of iron borides [1]. This thermochemical treatment is widely used to improve the surface hardness, the tribological properties and the corrosion resistance of ferrous alloys [2-5]. The boriding treatment is carried out in the temperature range of 800-1050°C for a treatment time ranging from 0.5 to 12 h. The boriding medium can be solid, liquid, plasma and gas.

The boride layer obtained on the ferrous alloys is composed of two kinds of iron borides. FeB is the outer layer while Fe_2B is the inner one [6, 7]. A transition zone can exist in the alloyed steels, located between the boride layer and the substrate. Certain elements such as silicon and carbon which are not dissolved in the iron borides are held in solid solution forming this transition zone. The morphology of the (boride layer/substrate) interface is affected by the presence of alloying elements [8-11]. The (boride layer/substrate) exhibits a saw tooth morphology for Armco iron and carbon steels [12-14] whereas this interface tend to be flat in the case of high -alloy steels [15, 16].

The aim of the present study was to investigate the solid boriding of a high alloyed steel (X200CrMoV12) in the temperature range of 900-1000°C. The generated boride layers were characterized by Optical microscopy (OM), Scanning electron microscopy (SEM) coupled to EDS analysis and XRD analysis. The growth kinetics of boride layers was investigated by estimating the boron activation energy for the X200CrMoV12 steel

2. Experimental details
2.1 The boriding treatment

The X200CrMoV12 steel was selected for the pack-boriding treatment. Its chemical composition in mass (%) is given in Table 1.
The samples to be borided were cut in cubic form with dimensions of 10x10x10 mm^3. They were

---

* Corresponding author: keddam@yahoo.fr

ground using 180 to 400 grit papers in sequence. They were finally cleaned with acetone to remove grease and dirt. The boriding treatment was realized in a sealed stainless steel container placed in an electrical resistance furnace. The samples were embedded in the powder mixture composed of: 5%B_4C (boriding source), 5%$NaBF_4$ (activator) and 90% SiC (diluant). Afterwards, the samples were heated in an electrical resistance furnace at 900, 950 and 1000°C for 2, 4 and 6 h, respectively. When the treatment was finished, the borided samples were removed from the furnace and cooled in air.

Table 1. *Chemical composition (in mas.%) of the X200CrMoV12 steel.*

C	Cr	Mo	V	Mn	W	Si	Ni	Cu	P	S
2	12.46	0.54	0.65	0.37	0.28	0.2	0.26	0.1	0.02	0.001

2.2 Characterization of the borided samples

The cross-sections of the borided samples were examined by an optical microscope (Carl Zeiss Axio Teck 100 type). The morphology of the boride layers was observed by scanning electron microscopy using the JOEL-5600LV microscope. The presence of iron borides at the surface of borided samples was verified by means of an X-ray diffractometer (PHILIPS X'PERT PRO MPD) with a CuKα radiation source with a wavelength of a 0.154 nm. To identify the phases from the diffraction peaks, the data from the JCPDS database were used [17].

3. Results
3.1. Microstructural observations of the boride layers.

Figure 1 shows the optical image of the surface of unborided X200CrMoV12 steel, etched by Nital (3%). It reveals the presence of carbides inside the ferritic matrix after a heat treatment (quenching followed by tempering). These carbides are of different size and shape.

Figure 2 shows the optical micrographs of cross-sectional views of the borided samples from X200CrMoV12 steel, at different temperatures (900, 950 and 1000° C) during 6 h of treatment. The formed boride layers are compact and homogenous exhibiting a flat diffusion front due to the presence of alloying elements. The obtained microstructure revealed the presence of the both layers FeB and Fe_2B. The two iron borides can be distinguished by a difference in contrast (Figure 2 c).

Figure 3 gives the SEM micrograph of the cross-section of borided layers formed on the X200CrMoV12 steel at 1000°C for 6 h. The total boride layer is composed of an outer layer FeB and an
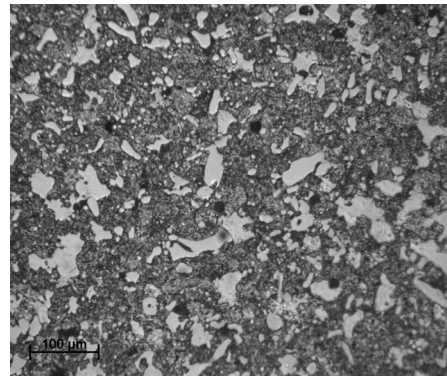
Figure 1. *Optical image of the initial microstructure of X200CrMoV12 steel after a heat –treatment (quenching followed by tempering).*

a)

b)

c)
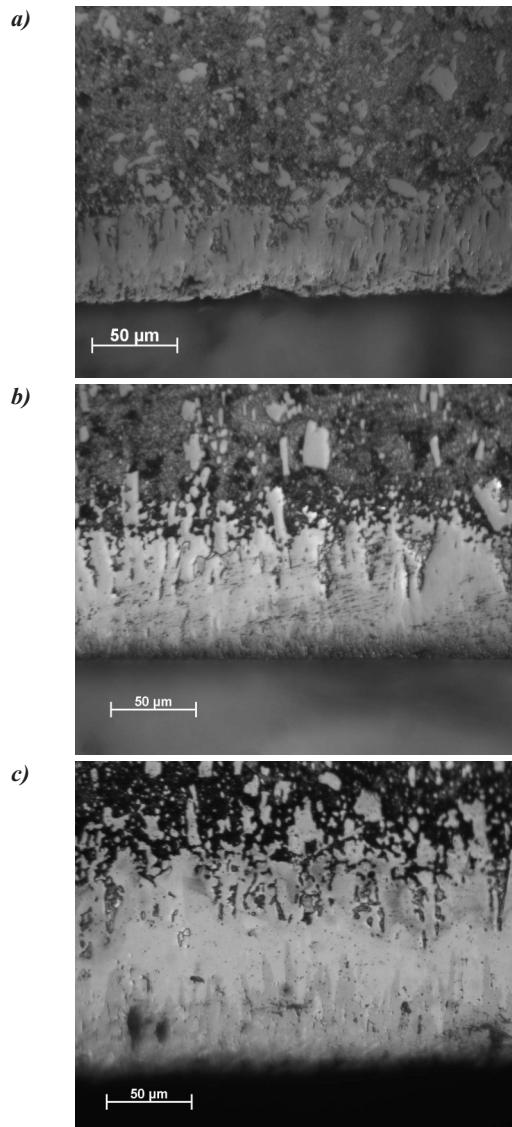
Figure 2. *Optical micrographs of the cross-sections of the borided layers formed on the 200CrMoV12 steel during 6 h at different temperatures: (a) 900°C, (b) 950°C and (c) 1000°C.*
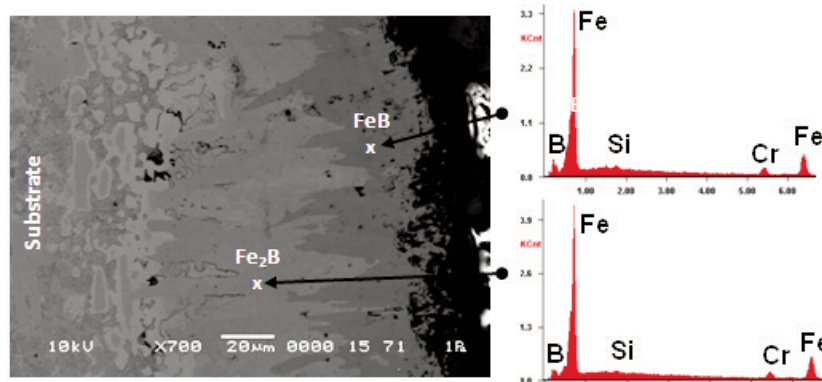
Figure 3. SEM image coupled to the EDS analysis of the cross-section of borided layers formed on the 200CrMoV12 steel at 1000°C for 6 h of treatment.

inner layer Fe$_2$B showing also a difference in contrast. The EDS analysis points out the presence of four elements: (Fe, Cr, Si and B) in the FeB and Fe$_2$B layers.

3.2 XRD analysis

Figure 4 gives the XRD pattern of the borided sample at 1000°C for 6 h of treatment .It indicates the presence of two iron borides (FeB and Fe$_2$B) at the surface of borided X200CrMoV12 steel. To confirm the presence of these two iron borides, the two files from the JCPDS database [17] were used: (00-032-0463 for Fe$_2$B and 00-036-1332 for FeB).The FeB phase is diffracted according to the crystallographic planes (021), (120) and (212), while the Fe$_2$B phase is identified by the diffracting planes (211), (002) and (112).
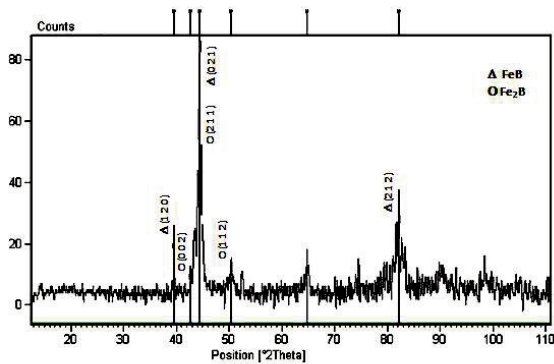
Figure 4. XRD pattern obtained at the surface of borided X200CrMoV12 steel at 1000°C for 6 h of treatment.

3.3. Determination of the activation energy of boron diffusion

The growth kinetics of boride layers is controlled by the boron diffusion into the substrate. The time dependence of boride layer thickness follows a parabolic growth law [18-20]:

$$u = k'\sqrt{t} \tag{1}$$

with $k' = k\sqrt{D}$

where u is the boride layer thickness, k a dimensionless constant at a given temperature, D the diffusion coefficient of boron in the boride layer and t the boriding time. The time dependence of boride layer thickness for increasing temperatures is given in Figure 5.

It is seen that the boride layer varies linearly with $\sqrt{t}$, which proves that the growth kinetics of boride layer is governed by the diffusion phenomenon of boron atoms.
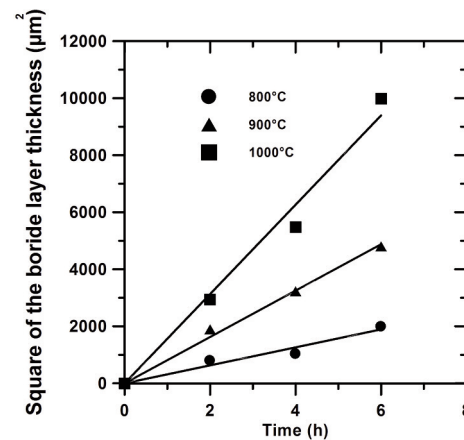
Figure 5. Evolution of the square of boride layer thickness versus time for increasing temperatures.

The relationship between the parabolic growth constant k' and the boriding temperature T in Kelvin, can be expressed by an Arrhenius-type equation as follows:

$$k' = k\sqrt{D_0 \exp(-\frac{Q}{RT})} \tag{2}$$

Where D_0 is the diffusion coefficient of boron extrapolated at a value of $1/T=0$. The Q parameter is the activation energy which indicates the amount of energy (kJ mol^{-1}) required for the reaction to occur, and R is the ideal gas constant (R=8.314 J mol $^{-1}$ K^{-1}). Taking the natural logarithm of Eq. 2, one gets Eq.(3):

$$\ln(k'^2) = \ln(k^2) + \ln(D_0) - (\frac{Q}{RT}) \qquad (3)$$

The activation energy Q can be easily deduced from the slope of the curve relating $\ln(k'^2)$ to the inverse of temperature. Figure 6 gives the temperature dependence of natural logarithm of the square of parabolic growth constant k'^2.

The reported values of the activation energies [13, 21-26] of the borided steels are listed in Table 2 together with the value of boron activation energy (199.37 kJ mol^{-1}) estimated in this work.
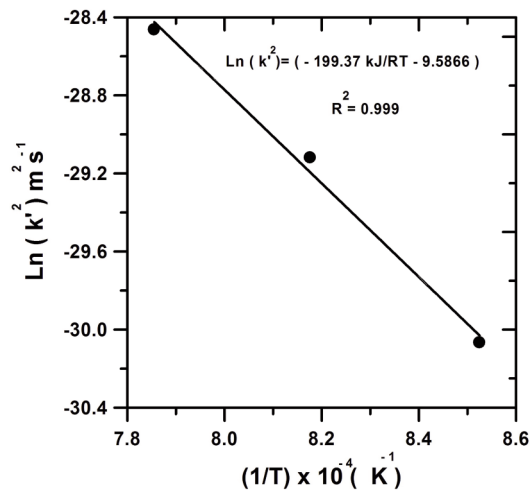
Figure 6. Temperature dependence of the square of parabolic growth constant.

Table 2. Values of boron activation energies obtained in the case of borided steels by different methods.

Material	Boriding method	Q (kJ mol^{-1})	References
AISI 304	Salt Bath	253.35	[21]
AISI H13	Salt bath	244.37	[21]
AISI4140	Paste	168.5	[22]
AISI H13	Powder	186.2	[23]
AISI 1040	Powder	168	[24]
C35	Powder	153.1	[13]
AISI 51100	Plasma	106	[25]
AISI 304	Plasma Paste Boriding	123	[26]
X200CrMoV12	Powder	199.37	Present study

3.4. Prediction of the boride layer thickness with a regression model

A full factorial design with 2 factors at 3 levels [27] was used to predict the boride layer thickness as a function of the boriding parameters (time and temperature).

By use of this approach, Eq. (4) was obtained as follows:

$$u(t,T) = -86.094 + 0.11766 \times T - 62.262 \times t + 0.073250 \times t \times T \quad (4)$$

Where t is the boriding time (h) and T the temperature in degree Celsius. Eq. (4) can be used to plot the iso-thickness diagram shown in Figure 7.
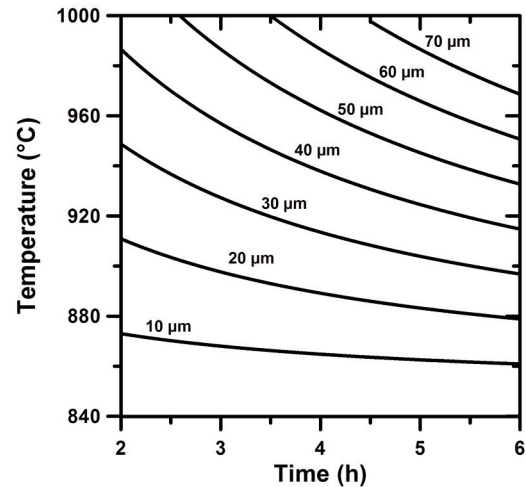
Figure 7. Iso-thickness diagram describing the evolution of the boride layer thickness as a function of the boriding parameters.

Table 3 compares between the experimental values of borided layers thicknesses and the predicted values using Eq. (4) in the temperature range of 900-1000°C. A good agreement was then observed between these two set of data with a maximum standard deviation of about $\pm$ 2.90 μm.

Table 3. Comparison between the experimental values of borided layers thicknesses and those given by the regression model (Eq.4) in the temperature range of 900-1000°C.

T (°C)	t (h)	Borided layer thickness (μm)	
		Exp.	Simul.
900	2	28.2	27.1
	4	32.1	34.4
	6	44.6	41.7
950	2	43.5	40.3
	4	56.8	55,0
	6	69.3	69.6
1000	2	54.2	53.5
	4	74	75.5
	6	99.9	97.5

4. Discussion

The X200CrMoV12 steel was pack-borided in the temperature range of 900–1000°C for studying the boriding kinetics. The microstructure of boride layer formed on the X200CrMoV12 steel is composed of two kinds of layers FeB and Fe$_2$B. Their existence was confirmed by XRD analysis.

The OM and SEM observations showed the formation of total boride layers with a less saw-tooth morphology. So, the (boride layer/ substrate) interface looks to be smooth due to the effect of alloying elements in the matrix [16]. The EDS analysis puts into evidence that chromium can enter into the iron borides lattices to form the complex borides such as (Fe, Cr)$_2$B and (Fe, Cr)B [9-11].

The kinetics of formation of the total boride layers followed a parabolic growth law. The total boride layer thickness increased with an increase in the boriding temperature. Basing on our experimental data, the boron activation energy of the X200CrMoV12 steel was estimated as 199.37 kJ mol^{-1}. It is interpreted as the required energy to stimulate the boron diffusion through the [001] preferred direction [12].

This value was then compared with the results found in the literature. It is seen that the determined values of boron activation energies [13, 21-26] are found to be dependent on the boriding method and on the chemical composition of the substrates as well as on the mechanism of boron diffusion into the substrate surface.

A full factorial design with 2 factors at 3 levels [27] was used to predict the boride layer thickness as a function of the boriding parameters (time and temperature). A simple equation, based on the regression model, was obtained for plotting the iso-thickness diagram.

This regression model was also validated by comparing the experimental total boride layers thicknesses with the predicted values in the temperature range of 900-1000°C. A good agreement was then obtained between the experimental results and the predicted values.

5. Conclusion

The pack-boriding of X200CrMoV12 steel was investigated in the temperature range of 900-1000°C by varying the treatment time from 2 to 6 h. The following concluding points can be drawn from the present study:

The morphology of (boride layer/ substrate) interface exhibited a flat front. The total boride layer thickness reached a value of 99.9 μm for 6 h of treatment at 1000°C, while it was only 28.2 μm for 2 h at 900° C.

The SEM observations revealed the presence of both layers (FeB and Fe$_2$B). The existence of these two iron borides were confirmed by XRD analysis.

The kinetics of formation of boride layers followed a parabolic relationship.

The boron activation energy was estimated as 199.37 kJ mol^{-1} for the X200CrMoV12 steel. It is interpreted as the required energy to stimulate the boron diffusion through the [001] preferred direction.

An iso-thickness diagram relating the total boride layer thickness to the two boriding parameters (time and temperature) was established to be used a simple tool to select the optimum values of total boride layer thickness according to the industrial application of X200CrMoV12 steel.

References

[1] A.K. Sinha, J. Heat Treatment, 4 (1991), 437-447.

[2] R. Chatterjee-Fisher, Boriding and diffusion metallizing. In: Sundarshan TS, editor. Surface modification technologies. NewYork: Marcel Dekker Inc.; 1989. p. 567 [chapter 8].

[3] G. Çelebi, M.Ipeck, C. Bindal, A.H.Űcisik, Mater. Forum, 29 (2005) 456-460.

[4] V.Jain, G.Sundararajan, Surf. Coat. Technol., 149 (2002) 21-26.

[5] S. Şahin, J. Mater. Process Tech., 209 (2009) 1736-1741.

[6] V.P. Glukhov, Boronizing steel, Sov. Powder Metall. Met. Ceram., 4 (76) (1969) 278–283.

[7] C. Martini, G. Palombarini, G. Poli, D. Prandstraller, Wear 256 (2004) 608–613.

[8] P. Goeuriot, R. Fillit, F. Thevenot, J. H. Driver and H. Bruyas, Mater. Sci. Eng., 55 (1982) 9 – 19.

[9] V.I. Dybkov, W. Lengauer, K. Barmak, J. Alloy. Compd., 398 (2005) 113–122.

[10] V. I. Dybkov, J. Mater. Sci., 42 (16) (2007) 6614-6627.

[11] V. I. Dybkov, W. Lengauer, P. Gas, J. Mater. Sci. 41 (2006) 4948–4960.

[12] C.M. Brakman, A.W.J. Gommers, E.J. Mittemeijer, J. Mater. Res., 4 (1989) 1354-1370

[13] B. Bouarour, M. Keddam, O. Allaoui, O.Azouani, Metall. Res. Technol. 111 (2014) 67–73.

[14] Z. Nait Abdellah, M. Keddam, R. Chegroune, O. Azouani, O. Allaoui, A. Elias, Matériaux et Techniques, 100 (2012) 271-278.

[15] I. Campos-Silva, M. Ortiz-Domínguez, O. Bravo-Bárcenas, M. A. Doñu-Ruiz, D.Bravo-Bárcenas, C. Tapia-Quintero , M.Y. Jiménez-Reyes, Surf. Coat. Technol., 205 (2010) 403-412.

[16] I. Campos-Silva, M. Ortiz-Domínguez, C. Tapia-Quintero, G. Rodriguez-Castro, M.Y. Jimenez-Reyes, E. Chavez-Gutierrez, J. Mater. Eng. Perform., 21 (2012) 1714-1723.

[17] JCPDS- International Centre for Diffraction Data, PCPDF WIN, Version 202 (1999).

[18] N. Ucar, O. B. Aytar, A. Calik, Mater.Technol., 46 (2012) 621–625

[19] X. Tian, Y. L. Yang, S. J. Sun, J. An, Y. Lu, Z. G. Wang,

J. Mater. Eng. Perform., 18 (2009) 162

[20] L. Xu, X. Wu, H. Wang, J. Mater. Sci. Technol., 23 (2007) 525.

[21] S. Taktak, Mater. Sci., 41 (2006) 7590–7596.

[22] Z. Nait Abdellah, M. Keddam, A. Elias, Int. J. Mater. Res., 104 (2013) 260-265.

[23] K. Genel, Vacuum 80 (2006) 451.

[24] I. Uslu, H. Comert, M.Ipek, F.G. Celebi, O. Ozdemir, C. Bindal, Mater. Design, 28 (2007) 1819

[25] M. Ipek, G. Celebi Efe, I. Ozbek, S. Zeytin, and C. Bindal, J. Mater. Eng. Perform. 21 (2012) 733-738

[26] J.H. Yoon, Y.K. Jee, S.Y, Lee, Surf. Coat. Technol., 112 (1999) 71–75.

[27] J. Goupy, Plans d'expériences pour surfaces de réponses, Edition Dunod, (2001).